



SEISMIC WAVES IN 3-D SEDIMENTARY BASINS DUE TO POINT SOURCE

YUZO SHINOZAKI^{*1} and KAZUHIRO YOSHIDA^{*2}

^{*1}Department of Architectural Engineering, Kyoto University, Kyoto, JAPAN

^{*2}Ohsaki Research Institute, Shimizu Corp., Tokyo, JAPAN

ABSTRACT

A direct three-dimensional boundary element method is applied to evaluate seismic waves in three-dimensional sedimentary basin for both incident plane waves such as SH, P, SV, and Rayleigh waves, and incident waves generated from a point source. We have utilized the Green's functions for an elastic half-space medium to formulate boundary integral equations in terms of displacements and tractions at the medium interface. Frequency responses of surface displacement amplitudes of a semi-spherical sedimentary basin for SH waves propagating nonvertically to the surface show good agreements with those results evaluated with the solution (Sanchez-Sesma *et al.*, 1989) based on wave function expansions and an azimuthal decomposition. Time domain responses as well as frequency domain responses are presented for different depths of the sedimentary basin and for different types of incident waves.

KEYWORDS

Sedimentary basin; boundary element method; site effects ; three-dimensional model; Green function; strong ground motion; point source; earthquake damage

INTRODUCTION

It has been recognized that the dynamic behavior of a structure during an earthquake is considerably affected by the geologic formation and the dynamic property of the soil medium. In particular, the topographic irregularities in the soil medium seem to have a tremendous effect on the characteristics of the earthquake ground motion, together with the associated structural damage of the building. There have been many theoretical studies about the elastic wave propagation in or around such geologic and topographic irregularities of the soil medium.

But there have been a few studies (Horike *et al.*, 1990; Shinozaki and Yoshida, 1994; Sanchez-Sesma and Luzon, 1995) about seismic waves in a 3-D sedimentary basin whose shape of medium interface is arbitrarily shaped. In the present study, we examine seismic waves in a 3-D sedimentary basin for both incident plane waves such as SH, P, SV, and Rayleigh waves, and incident waves generated from a point source. A direct boundary element method is applied to evaluate seismic waves in a 3-D sedimentary basin. We have utilized the Green's functions for an elastic half-space medium calculated by one of the authors, who verified the accuracy of the Green's functions through comparison of the numerical results with those obtained by other method. Since the boundary conditions at the free surface of elastic media are automatically satisfied, the direct 3-D boundary element method is precisely formulated through those Green's functions based on the boundary conditions along an arbitrarily shaped medium interface. Time domain responses as well as frequency domain responses are presented for different depths of the sedimentary basin and for different types of incident waves.

METHOD OF ANALYSIS

Geometry of the problem is shown in Figure 1. A sedimentary basin is assumed to be a 3-D model (denoted by medium 1), which is characterized by mass density, ρ_1 , compressional wave velocity, α_1 , and shear wave velocity, β_1 . Medium 1 is surrounded by a half-space medium (denoted by medium 2), which is characterized by mass density, ρ_2 , compressional wave velocity, α_2 , and shear wave velocity, β_2 . An interface between the media 1 and 2 is denoted by S and perfect bonding along the interface is understood. The material of them is assumed to be linearly elastic, homogeneous and isotropic.

The total wave field in the surrounding half-space, $\mathbf{u} [= \{u_x, u_y, u_z\}^T]$ is given by

$$\mathbf{u} = \mathbf{u}^{sc} + \mathbf{u}^{in}, \quad (1)$$

where the superscript sc denotes the wave field scattered from the medium interface between the sedimentary basin and surrounding half-space, and the superscript in denotes the incoming wave field which includes the incident waves and their reflections from the free surface.

To derive the boundary integral representations, we start with Betti's reciprocity theorem written in the following form:

$$\int \int \int_{\Omega} (f_i^B u_i^A - f_i^A u_i^B) d\Omega = \int \int_S (u_i^B p_i^A - u_i^A p_i^B) dS. \quad (2)$$

In the above u_i^A and p_i^A represent the i -th components of displacement and surface traction due to body force f_i^A , while u_i^B and p_i^B are the i -th components of displacement and surface traction due to body force f_i^B in region Ω .

In equation (2) we employ the following sets of functions,

$$\{ u_i^A(\mathbf{x}), p_i^A(\mathbf{x}) \} = \{ u_i^{sc}(\mathbf{x}), p_i^{sc}(\mathbf{x}) \}, \quad (3a)$$

$$\{ u_i^B(\mathbf{x}), p_i^B(\mathbf{x}) \} = \{ G_{ij}(\mathbf{x}; \mathbf{x}^*), H_{ij}(\mathbf{x}, \mathbf{n}; \mathbf{x}^*) \}, \quad (3b)$$

in which $G_{ij}(\mathbf{x}; \mathbf{x}^*)$ and $H_{ij}(\mathbf{x}, \mathbf{n}; \mathbf{x}^*)$ are the i -th components of displacement and traction at \mathbf{x} due to a point force in the j -th direction at \mathbf{x}^* , and \mathbf{n} is a unit outward normal of the boundary S . In this study we employ as $G_{ij}(\mathbf{x}; \mathbf{x}^*)$ and $H_{ij}(\mathbf{x}, \mathbf{n}; \mathbf{x}^*)$, the Green's functions and corresponding traction functions developed by Yoshida and Kawase(1988).

After substitution of equation (3) to equation (2) and exchange of \mathbf{x} for \mathbf{x}^* as well as of subscript $\{j\}$ for subscript $\{i\}$, we get the fundamental equation of boundary integral representation as follows,

$$u_i^{sc}(\mathbf{x}^*) = \int \int_S \left\{ G_{ji}(\mathbf{x}; \mathbf{x}^*) \cdot p_j^{sc}(\mathbf{x}, \mathbf{n}) - H_{ji}(\mathbf{x}, \mathbf{n}; \mathbf{x}^*) \cdot u_j^{sc}(\mathbf{x}) \right\} dS. \quad (4)$$

In the direct BEM formulation, we need the expression in which a point \mathbf{x}^* lies on the boundary S . This can be obtained by considering the limit $\mathbf{x}^* \rightarrow \mathbf{x}$

$$C \cdot u_i^{sc}(\mathbf{x}^*) = \int \int_S \left\{ G_{ji}(\mathbf{x}; \mathbf{x}^*) \cdot p_j^{sc}(\mathbf{x}, \mathbf{n}) - H_{ji}(\mathbf{x}, \mathbf{n}; \mathbf{x}^*) \cdot u_j^{sc}(\mathbf{x}) \right\} dS. \quad (5)$$

where, C is a constant determined by the boundary shape around \mathbf{x}^* and equal to 1/2 in case of a smooth boundary. This equation shows that the boundary values are directly related to each other through the Green's functions. Note that the integration contains a singularity in $G_{ij}(\mathbf{x}; \mathbf{x}^*)$ and $H_{ij}(\mathbf{x}, \mathbf{n}; \mathbf{x}^*)$.

On the other hand, the incoming wave field should satisfy the equation

$$(1 - C) \cdot u_i^{in}(\mathbf{x}^*) = \int \int_S \left\{ -G_{ji}(\mathbf{x}; \mathbf{x}^*) \cdot p_j^{in}(\mathbf{x}, \mathbf{n}) + H_{ji}(\mathbf{x}, \mathbf{n}; \mathbf{x}^*) \cdot u_j^{in}(\mathbf{x}) \right\} dS. \quad (6)$$

From these two equations and equation (1) we obtain the following BEM equation for the surrounding medium (medium 2).

$$C \cdot u_i^{(2)}(\mathbf{x}^*) = \int \int_S \left\{ G_{ji}^{(2)}(\mathbf{x}; \mathbf{x}^*) \cdot p_j^{(2)}(\mathbf{x}, \mathbf{n}) - H_{ji}^{(2)}(\mathbf{x}, \mathbf{n}; \mathbf{x}^*) \cdot u_j^{(2)}(\mathbf{x}) \right\} dS + u_i^{in}(\mathbf{x}^*). \quad (7)$$

Following the same procedure, we obtain the following BEM equation for the interior region (medium 1).

$$(1 - C) \cdot u_i^{(1)}(\mathbf{x}^*) = \int \int_S \left\{ -G_{ji}^{(1)}(\mathbf{x}; \mathbf{x}^*) \cdot p_j^{(1)}(\mathbf{x}, \mathbf{n}) + H_{ji}^{(1)}(\mathbf{x}, \mathbf{n}; \mathbf{x}^*) \cdot u_j^{(1)}(\mathbf{x}) \right\} dS, \quad (8)$$

where, the superscript (m) ($m = 1, 2$) denotes the medium number. Equations (7) and (8) are combined using the boundary conditions prescribed by,

$$\begin{aligned} u_j^{(1)}(\mathbf{x}) &= u_j^{(2)}(\mathbf{x}) \\ p_j^{(1)}(\mathbf{x}, \mathbf{n}) &= p_j^{(2)}(\mathbf{x}, \mathbf{n}). \end{aligned} \quad (9)$$

To solve equations (7) and (8), the discretization scheme of both boundary shape and boundary values $u_j(\mathbf{x})$ and $p_j(\mathbf{x}, \mathbf{n})$ should be introduced in the same manner as the finite element method. The simplest boundary element is a constant-value element with fixed slope, which allows to express the integral equation by means of

$$C \cdot u_i(n) = \sum_{m=1}^M \tilde{G}_{ji}(m; n) \cdot p_j(m) - \sum_{m=1}^M \tilde{H}_{ji}(m; n) \cdot u_j(m), \quad (n = 1, M). \quad (10)$$

In this equation, M is the total number of elements and $\tilde{G}_{ji}(m; n)$ and $\tilde{H}_{ji}(m; n)$ are the element integrations over the surface of m -th element S_m expressed by

$$\tilde{G}_{ji}(m; n) = \int \int_{S_m} G_{ji}(\mathbf{x}; \mathbf{x}_n) ds_m \quad (11a)$$

$$\tilde{H}_{ji}(m; n) = \int \int_{S_m} H_{ji}(\mathbf{x}; \mathbf{x}_n) ds_m. \quad (11b)$$

Since $G_{ji}(\mathbf{x}; \mathbf{x}_n)$ and $H_{ji}(\mathbf{x}; \mathbf{x}_n)$ are proportional to the singular functions $1/r$ and $1/r^2$, respectively, where r is the distance between a source and receiver, namely, $r = |\mathbf{x} - \mathbf{x}_n|$, when m coincides with n , equations (11) should be accurately evaluated with the aid of efficient methods. In this study we dealt with those singularities of Green's functions and corresponding tractions using the method proposed by Hayami and Brebbia(1988).

By combining equations for different n we obtain the final simultaneous linear equations to be solved for the unknown boundary values as follows,

$$\begin{pmatrix} [\mathbf{H}]^{(2)} & [\mathbf{G}]^{(2)} \\ [\mathbf{H}]^{(1)} & [\mathbf{G}]^{(1)} \end{pmatrix} \begin{pmatrix} \mathbf{u} \\ \mathbf{p} \end{pmatrix} = \begin{pmatrix} \mathbf{u}^{in} \\ \mathbf{0} \end{pmatrix}, \quad (12)$$

where \mathbf{u} and \mathbf{p} represent unknown vectors of displacement and traction along the boundary S , respectively, and \mathbf{u}^{in} is the incoming wave field vector. And $[\mathbf{G}]^{(j)}$ and $[\mathbf{H}]^{(j)}$ ($j = 1, 2$) represent coefficient matrices whose elements are evaluated with equations (11). Once \mathbf{u} and \mathbf{p} are numerically solved, then displacements at any point in the medium can be calculated by the discretized form of equation (7) or (8).

It is easily seen that it is a formidable task to evaluate such element integrations as shown in equations (11), since they are composed of Green's functions for a half-space medium, *i.e.*, medium 1 or medium 2, which represent themselves infinite integrals difficult to compute accurately. If we assume to analyze an axisymmetric sedimentary basin, we could reduce significantly computational cost in evaluating equations (12) following the method proposed by Au and Brebbia(1983).

NUMERICAL RESULTS

The material properties of the sedimentary basin are normalized with respect to those of the half-space. The normalized frequency η is defined as $\eta = 2a/\lambda$ where λ is the wavelength of shear wave in the half-space and a is the radius of the sedimentary basin.

First we show some frequency domain responses of a semi-spherical sedimentary basin due to nonvertically propagating SH waves (Sanchez-Sesma *et al.*, 1989) to illustrate some verification of the present method. Figure 2 shows surface displacement amplitude u_y versus the normalized frequency η , normalized by the amplitude of incident SH waves, for the central site of a semi-spherical sedimentary basin due to an incident plane SH waves whose incident angle is equal to 30° . Material properties for media 1 and 2 are assumed to be the same values as those of Sanchez-Sesma *et al.*(1989) and be related by $\beta_1 = 0.45 \beta_2$ and $\rho_1 = \rho_2$ with Poisson's ratios $\nu_1 = 0.3$ and $\nu_2 = 0.25$, respectively. They are compared with the results of Sanchez-Sesma *et al.*(1989) indicated by solid circle. Fig. 2 shows very good agreements of the results. We calculated those responses of the semi-spherical sedimentary basin approximating the semi-spherical medium interface with 256 pieces of plane elements. Sanchez-Sesma *et al.*(1989) calculated the scattering of incident SH waves by a semi-spherical sedimentary basin using wave function expansion in terms of spherical Hankel or Bessel functions. Since each one of these wave functions does not itself satisfy the free-boundary conditions on the half-space surface, their method does not give exact solutions for the scattering of incident surface waves by

a 3-D sedimentary basin. It should be noted that the present method is applicable to the scattering of not only incident body waves but also incident surface waves by a 3-D sedimentary basin whose medium interface is arbitrarily shaped, because a boundary element problem is formulated in terms of exact Green's functions which satisfy the free-boundary conditions on the half-space surface.

From frequency domain results, we computed synthetic seismograms using the FFT algorithm. Figs. 3 show some examples of time history of surface displacement u_y for 79 sites along longitudinal section ($y = 0$) of a shallow sedimentary basin due to a point source located at (-10km, 0, 5km) excited in the y direction. It is noted that any surface displacement components such as u_z and u_x except u_y vanish along the x direction for the case of this excitation. Source time function is a Ricker wavelet with a characteristic period of 2.5 sec. It is assumed that the diameter and depth of the sedimentary basin are $a = 10\text{km}$ and $d = 1\text{km}$, respectively, and shear wave velocities of inclusion and half-space are $\beta_R = 0.9\text{km/sec}$ and $\beta_E = 2\text{km/sec}$ with Poisson's ratios $\nu_R = 0.3$ and $\nu_E = 0.25$, respectively. In each left side of the figures, the cross-section of the basin along the x direction is shown. Namely, Fig. 3a and Fig. 3b show the results of sedimentary basin for the case of inclined medium interface being 90° and 45° , respectively. It is seen that body waves, *i.e.*, SH waves, first arrive at the sites and then Love waves generated from the basin edge propagate forward along the longitudinal direction and propagate backward reflected from the other basin edge. It is also seen that though the body waves decay with the increase of source-receiver distance, Love waves do not decay because the material property of the basin is assumed to be a perfect elastic medium. It seems that the effect of angle of inclination of medium interface on the surface responses is small.

Figs. 4 show some examples of time history of surface displacements u_z and u_x for 79 sites along longitudinal section ($y = 0$) of a shallow sedimentary basin due to a point source located at (-10km, 0, 5km) excited in the x direction. The basin model assumed is the same as the one shown in Fig. 3b. Though any surface waves, *i.e.*, Rayleigh waves, propagating along the x axis are not clearly observed, the surface displacement u_z as well as u_x is more amplified near the basin edge nearest the point source.

Figs. 5 show some examples of time history of surface displacements u_z and u_x for 79 sites along longitudinal section ($y = 0$) of a shallow sedimentary basin due to a point source located at (-10km, 0, 5km) excited in the z direction. The basin model assumed is the same as the one shown in Fig. 3b. The similar wave propagation phenomena and total trend of variation of surface displacement amplification as shown in Fig. 4 are also observed in Fig. 5.

CONCLUSION

A direct 3-D boundary element method is applied to evaluate seismic waves in 3-D sedimentary basin for both incident plane waves such as SH, P, SV, and Rayleigh waves, and incident waves generated from a point source. We have utilized the Green's functions for an elastic half-space medium. Since the boundary conditions at the free surface of elastic media are automatically satisfied, the direct 3-D boundary element method is precisely formulated through those Green's functions based on the boundary conditions along a arbitrarily shaped medium interface. Frequency responses of surface displacement amplitudes of a semi-spherical sedimentary basin for SH waves propagating nonvertically to the surface show good agreements with those results evaluated with the solution (Sanchez-Sesma *et al.*, 1989) based on wave function expansions and an azimuthal decomposition.

Some time domain responses show that body waves, *i.e.*, SH waves, first arrive at the sites and then Love waves generated from the basin edge propagate forward along the longitudinal direction and propagate backward reflected from the other basin edge. They also show that though the body waves decay with the increase of source-receiver distance, Love waves do not decay because the material property of the basin is assumed to be a perfect elastic medium. It should be noted that the present method is applicable to the scattering of not only incident body waves but also incident waves generated from a point source by a 3-D sedimentary basin whose medium interface is arbitrarily shaped, because a boundary element problem is formulated in terms of exact Green's functions which satisfy the free-boundary conditions on the half-space surface.

REFERENCES

- Au, M. C. and C. A. Brebbia(1983). A three dimensional boundary element approach for rotationally problems, *Proc. Fifth Conf. Boundary Elements*, Hiroshima, Japan, Springer-Verlag, 915-928.
- Hayami, K. and C. A. Brebbia(1988). Quadrature methods for singular and nearly singular integrals in 3-D boundary element method, *Proc. 10th Int. Conf. on Boundary Elements*, Southampton, U.K., Springer-Verlag, 237-264.
- Horike, M., H. Uebayashi, and Y. Takeuchi(1990). Seismic response in three-dimensional sedimentary basin

due to S wave incidence, *J. Phys. Earth.*, **38**, 261-284.
 Sanchez-Sesma, F. J., L. E. Perez-Rocha, and S. Chavez-Perez(1989). Diffraction of elastic waves by three-dimensional surface irregularities. Part II, *Bull. Seism. Soc. Am.*, **79**, 101-112.
 Sanchez-Sesma, F. J. and F. Luzon (1995). Seismic response of three-dimensional alluvial valleys for incident P, S and Rayleigh waves, *Bull. Seism. Soc. Am.*, **85**, 269-284.
 Shinozaki, Y. and K. Yoshida(1994) Seismic waves in 3-D sedimentary basins, *Proceedings of 9th Japan Earthquake Engineering Symposium*, **1**, 325-330.
 Yoshida, K. and H. Kawase(1988). Dynamic interaction analysis of rigid embedded foundations by boundary element method, *Shimizu Technical Research Bulletin*, **7**, 33-47.

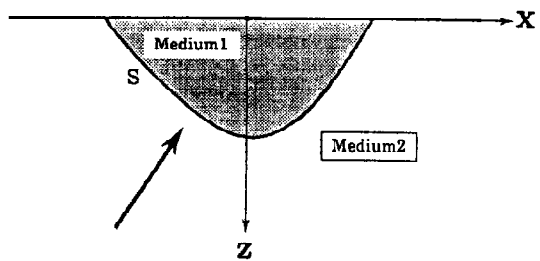


Fig. 1. Sedimentary basin model. The interior medium 1 enclosed by the boundary S has different material properties from the exterior medium 2 surrounding the boundary S.

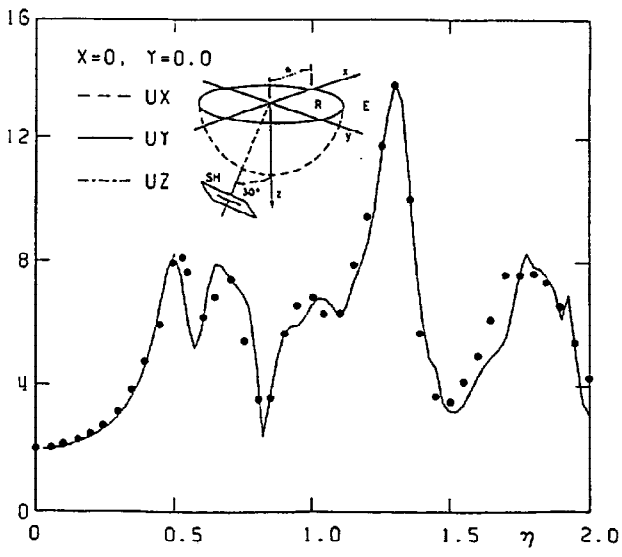


Fig. 2. Surface displacement amplitudes u_y for central point of a semi-spherical sedimentary basin with radius a versus normalized frequency η due to incident plane SH waves. Incidence of plane SH waves with incidence angle $\gamma = 30^\circ$. They are compared with the results of Sanchez-Sesma *et al.*(1989) indicated by solid circle.

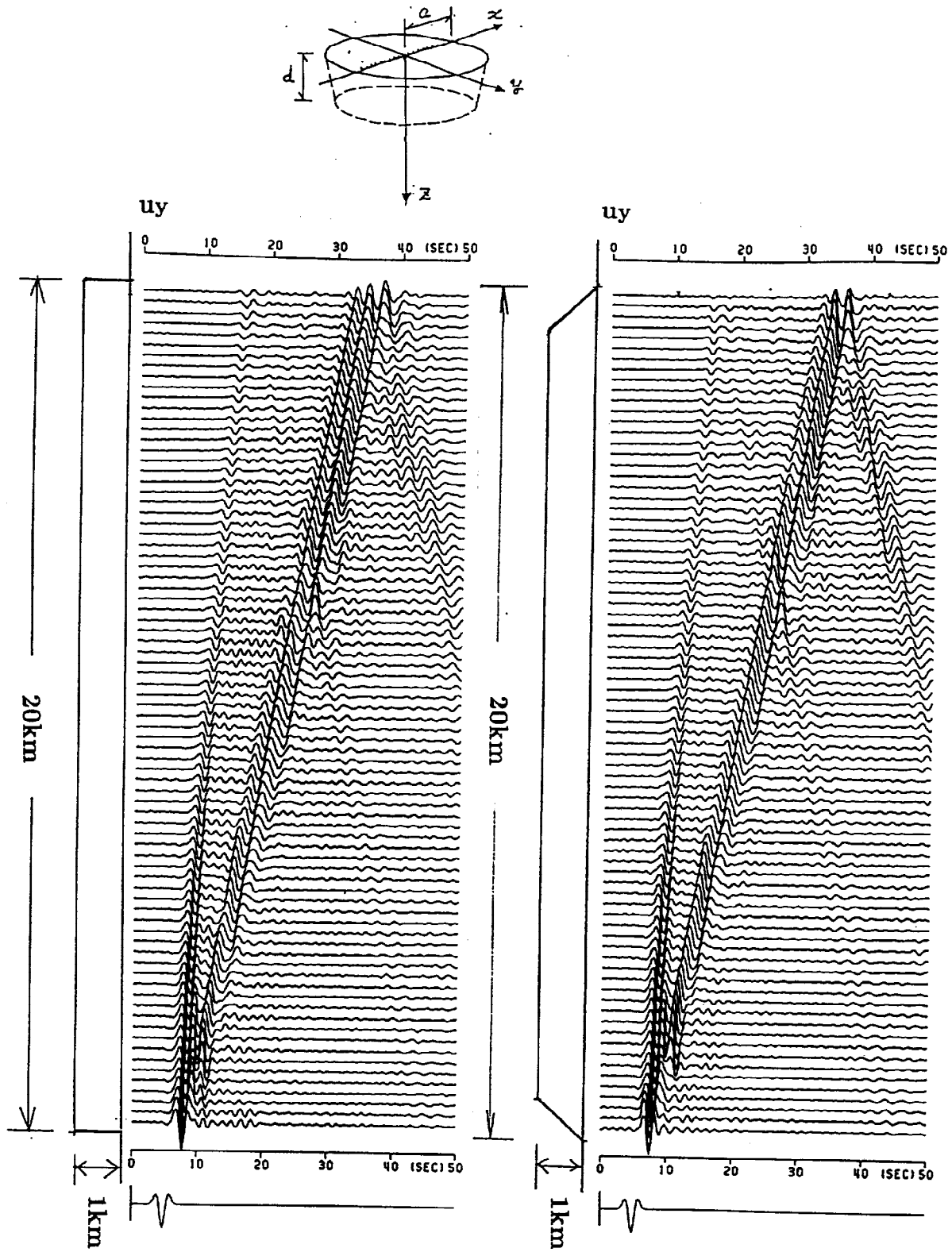


Fig. 3. Time-domain responses for surface displacement u_y at 79 sites equally spaced along the x axis of the 3-D sedimentary basin due to a point source excited in the y direction located at $(-10\text{km}, 0, 5\text{km})$. Source time function is a Ricker wavelet with a characteristic period of 2.5 sec.

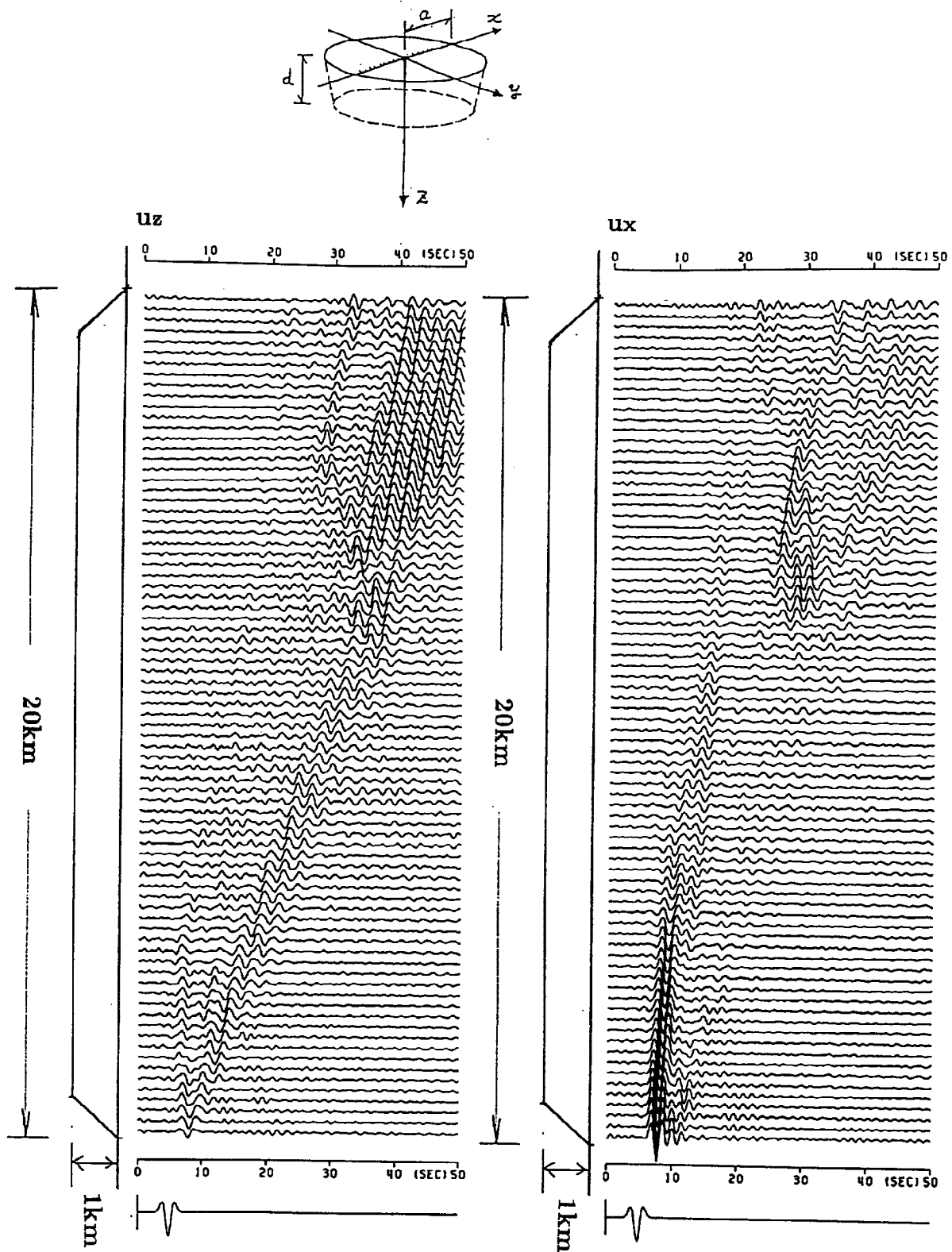


Fig. 4. Time-domain responses for surface displacements u_z and u_x at 79 sites equally spaced along the x axis of the 3-D sedimentary basin due to a point source excited in the x direction located at $(-10\text{km}, 0, 5\text{km})$. Source time function is a Ricker wavelet with a characteristic period of 2.5 sec.

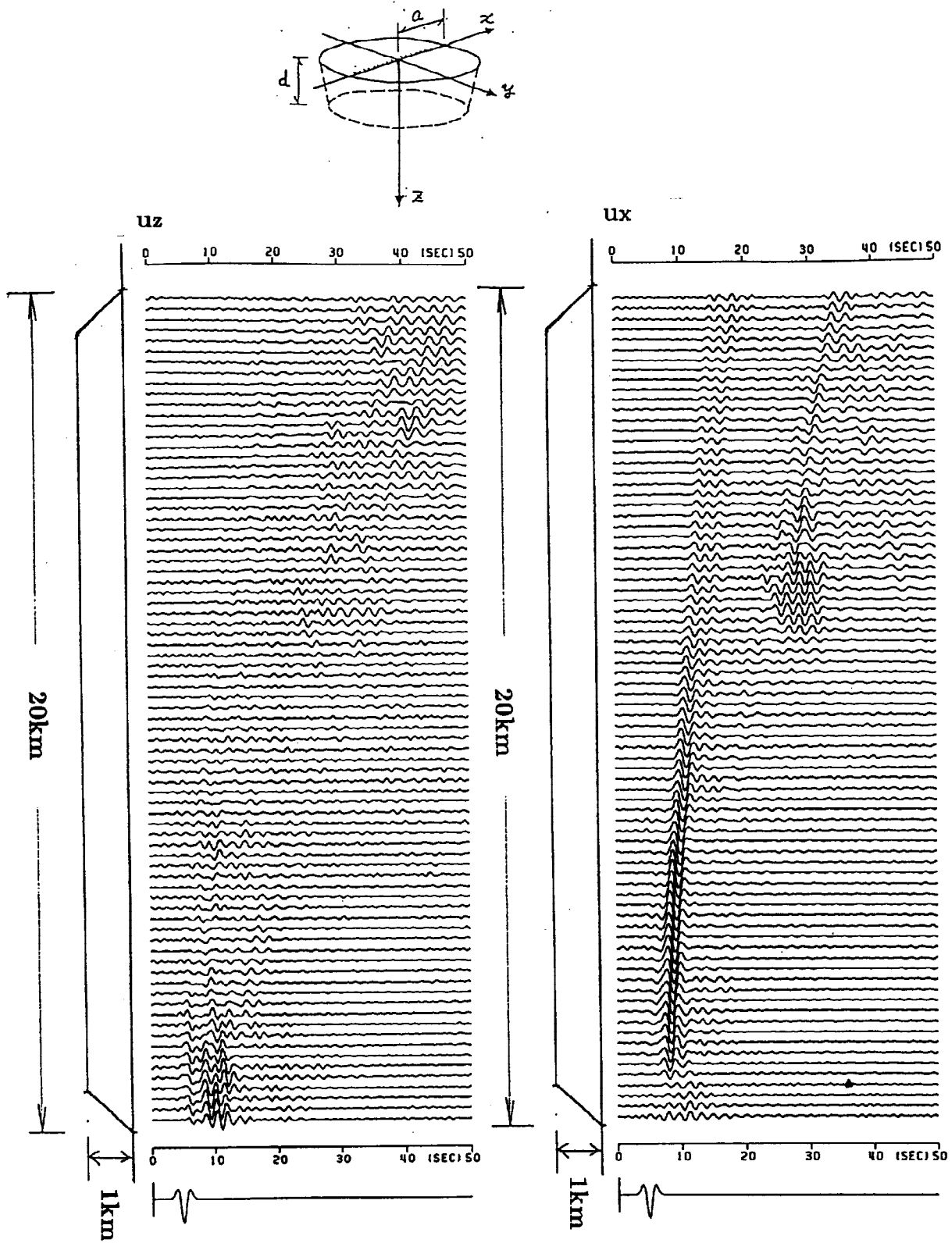


Fig. 5. Time-domain responses for surface displacements u_z and u_x at 79 sites equally spaced along the x axis of the 3-D sedimentary basin due to a point source excited in the z direction located at $(-10\text{km}, 0, 5\text{km})$. Source time function is a Ricker wavelet with a characteristic period of 2.5 sec.